1972-05

The fleet numerical weather central operational primitive-equation model

Kesel, Philip G.

Monthly Weather Review, Vol. 100, No. 5, pp. 360-373, May 1972.
http://hdl.handle.net/10945/45645

UDC 551.509.313:355.46

The Fleet Numerical Weather Central Operational Primitive-Equation Model

PHILIP G. KESEL—*U.S. Navy Fleet Numerical Weather Central, Monterey, Calif.*

FRANCIS J. WINNINGHOFF [1]—*U.S. Naval Postgraduate School, Monterey, Calif.*

ABSTRACT—The U.S. Navy Fleet Numerical Weather Central (FNWC), Monterey, Calif., five-layer, primitive-equation, atmospheric prediction model has been under development since late 1968 and became operational in September 1970. Seventy-two-hour prognoses are generated twice daily, requiring 2 hr per run.

The conservation forms of the difference equations are based on the Arakawa technique and are integrated, using a 381-km space step (at 60°N) and a 10-min time step, on sigma surfaces. Realistic mountains are used. Pressure-force terms are replaced by a single geopotential gradient on pressure surfaces synthesized locally to reduce inconsistent truncation error. Lateral diffusion is performed on forecast difference fields to prevent systematic distortions of sigma-surface state parameter distributions. Stress is applied at the lowest level. Restoration boundaries and centered time differencing are used. The integrations are restarted each 6 hr with a Euler-backward step to reduce solution separation.

The moisture and heat source and sink terms are modeled in a similar manner to those in the Mintz and Arakawa general circulation model. Terms representing evaporation and large-scale condensation, sensible heat exchange, a parameterization of cumulus convection and precipitation, and solar and terrestrial radiation are included. Dry convective adjustment precludes hydrostatic instability.

Initialization of the model is based on FNWCs Northern Hemisphere objective analyses of the state parameter structure from the surface to 50 mb. Nondivergent initial wind fields are obtained from solution of a linear balance equation.

The verification results are encouraging. The 36-hr sea-level pressure prognoses exhibit considerable skill. The model's ability to simulate the generation of new storms in the winter is noteworthy. Problems included the slow movement of small-scale features (truncation problem), need for improvement in description of the heating and friction, and a need for improved initialization.

1. INTRODUCTION

An important responsibility of the U.S. Navy Fleet Numerical Weather Central (FNWC), Monterey, Calif., is to provide numerical meteorological analyses and forecasts, on an operational basis, according to the needs of the U.S. Navy. In addition to this, FNWC is also responsible for the development and testing of meteorological techniques applicable to Navy prediction problems. Perhaps the most recent accomplishment of this development program has been the completion of the design and development, by the authors, of the FNWC five-layer, atmospheric prediction model based on the primitive equations. This development was initiated by Kesel under the direction of G. Haltiner and R. T. Williams at the Naval Postgraduate School early in 1968.

The model was initially programmed as a single-processor version to be executed in one of the two FNWC Control Data Corporation (CDC) 6500 computer systems.[2] In 1969, the emphasis was on boundary conditions, initialization procedures, the elimination of inconsistent truncation errors, the introduction of stress and diffusion terms, the inclusion of source and sink terms in the moisture and thermodynamic equations, and the stability of solutions. By early 1970, the development had reached a point at which the complete model was rather skillfully simulating the essential distributions of the state parameters for forecast periods from 1 to 3 days. Its ability to predict the generation of new storms was particularly encouraging, especially those storms that developed just off the east coast of Asia.

The FORTRAN-coded, single-processor model, however, required over 3 hr of computer time to output a set of 36-hr predictions. During the period from May to August 1970, the FNWC primitive-equation model was partitioned and programmed to run simultaneously in all four central processing units of the two CDC 6500 computers. The execution time for a 3-day forecast run has been reduced by a factor of 3:1 to just under 2 hr. At present, the four-processor model is being run to 72 hr twice daily.

The main purpose of this paper is to describe, in moderate detail, the FNWC four-processor, primitive-equation model. It is felt to be important to outline the approach taken to exploit the parallelism in the equation set, as well as to take advantage of the total system capability to make this model operationally useful.

Section 2 contains the description of the model. The special treatment of the heating and moisture source and sink terms is described in section 3. The four-processor model design is contained in section 4. Sections 5 and 6 are devoted to interim verification results and discussion of future model development, respectively. Appendixes 1

[1] Now affiliated with the Department of Meteorology, University of California, Los Angeles

[2] Mention of a commercial product does not constitute an endorsement.

and 2 contain the difference equations and the quantitative description of the heating terms, respectively.

2. MODEL DESCRIPTION

The governing differential equations, written in flux form, are similar to sets used by Smagorinsky et al. (1965) and Arakawa et al. (1969). The conservative-type difference equations are based on the Arakawa (1966) technique. The continuous equations are listed below. The complete finite-difference equations are given in appendix 1 in the form they are used in this model.

Momentum equation in the x-direction:

$$\frac{\partial \pi u}{\partial t}=-m^2\left[\frac{\partial}{\partial x}\left(\frac{uu\pi}{m}\right)+\frac{\partial}{\partial y}\left(\frac{uv\pi}{m}\right)\right]+\pi\frac{\partial(wu)}{\partial\sigma}+\pi vf-m\left(\pi\frac{\partial\phi}{\partial x}+RT\frac{\partial\pi}{\partial x}\right)+D_u+F_x. \quad (1)$$

Momentum equation in the y-direction:

$$\frac{\partial \pi v}{\partial t}=-m^2\left[\frac{\partial}{\partial x}\left(\frac{uv\pi}{m}\right)+\frac{\partial}{\partial y}\left(\frac{vv\pi}{m}\right)\right]+\pi\frac{\partial(wv)}{\partial\sigma}-\pi uf-m\left(\pi\frac{\partial\phi}{\partial y}+RT\frac{\partial\pi}{\partial y}\right)+D_v+F_y. \quad (2)$$

Thermodynamic energy equation:

$$\frac{\partial \pi T}{\partial t}=-m^2\left[\frac{\partial}{\partial x}\left(\frac{\pi uT}{m}\right)+\frac{\partial}{\partial y}\left(\frac{\pi vT}{m}\right)\right]+\pi\frac{\partial(wT)}{\partial\sigma}+H\pi+D_T+\frac{RT}{c_p\sigma}\left\{-w\pi+\sigma\left[\frac{\partial\pi}{\partial t}+m\left(u\frac{\partial\pi}{\partial x}+v\frac{\partial\pi}{\partial y}\right)\right]\right\}. \quad (3)$$

Moisture conservation equation:

$$\frac{\partial q\pi}{\partial t}=-m^2\left[\frac{\partial}{\partial x}\left(\frac{\pi uq}{m}\right)+\frac{\partial}{\partial y}\left(\frac{\pi vq}{m}\right)\right]+\frac{\pi\partial(wq)}{\partial\sigma}+Q\pi+D_q \quad (4)$$

where Q=moisture source/sink term.

Continuity equation:

$$\frac{\partial\pi}{\partial t}=-m^2\left[\frac{\partial}{\partial x}\left(\frac{u\pi}{m}\right)+\frac{\partial}{\partial y}\left(\frac{v\pi}{m}\right)\right]+\pi\frac{\partial w}{\partial\sigma}. \quad (5)$$

Hydrostatic equation:

$$\frac{\partial\phi}{\partial\sigma}=-\frac{RT}{\sigma}. \quad (6)$$

In the above equations, u is the x-direction wind component, v is the y-direction wind component, π is surface pressure, $w=-d\sigma/dt$ is vertical velocity, m is the map factor, T is temperature, f is the Coriolis parameter, ϕ is geopotential, q is specific humidity, H is the diabatic heating, F_x and F_y are the stress components, and the terms with Ds refer to the lateral diffusion for the quantity indicated by the subscript.

In appendix 1, the form of the finite-difference equations used requires that the horizontal advection terms conserve *kinetic energy*. In a strict sense, the difference form for the hydrostatic equation, which is energetically consistent, must be used. Such a form, along with a demonstration of the energy conserving properties, is given by Haltiner (1971) among others. However, the model used here does not use that form of the hydrostatic equation (cf. eq 21 and 22 in app. 1). The basic reason for using eq 21 and 22 was to reconcile the initial temperature, height, and surface pressure analyses with the forecast variables in the model. Experience does indicate that this leads to no perceptible ill effects for the time range of the forecasts.

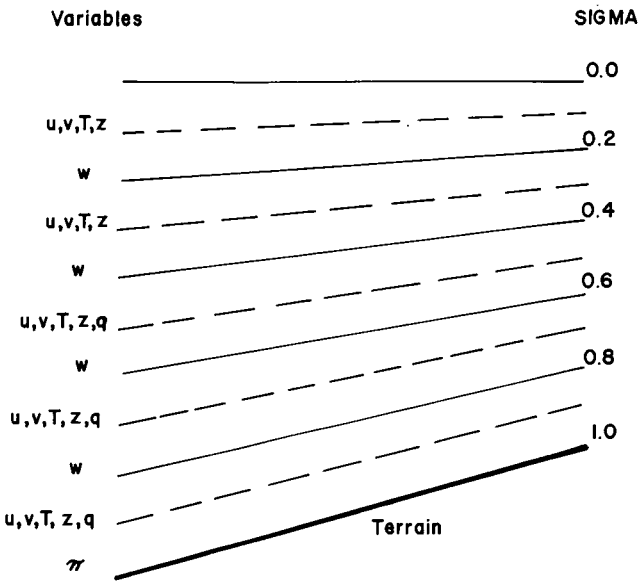

FIGURE 1.—Diagram of levels and variables. The terrain pressure, π, is carried at $\sigma=1.0$. The vertical velocity, w, vanishes at the top and bottom of the column.

a. Domain, Variables

Integrations are performed on Phillips' (1957) sigma surfaces in which pressure, p, is normalized with the underlying terrain pressure, π. The horizontal wind components, u, v; temperatures, T; and heights, z, are carried at levels where $\sigma=0.9$, 0.7, 0.5, 0.3, and 0.1. The moisture variable, q, is carried at the lower three of these surfaces. The vertical-velocity variable, w, is defined as $-d\sigma/dt$ and is calculated diagnostically from the continuity equation for the layer interfaces ($\sigma=0.8$, 0.6, 0.4, 0.2). All variables are carried at each point (i, j) of the horizontal grid (fig. 1).

The earth is mapped onto a polar stereographic projection of the Northern Hemisphere. In the calculation of the map factor and Coriolis parameter, the sine of the latitude is not permitted to take on values less than that value corresponding to 23° latitude. This restriction arose from the attempt in practice to produce more realistic appearing initial winds in the subtropics and Tropics and to allow use of the 10-min time step. The horizontal domain consists of a 59×59 subset of the standard 63×63 FNWC grid. The geographical Equator is an inscribed circle of the latter.

b. Time Differencing, Solution Separation

For all terms except lateral diffusion, friction, and heating, the centered time differencing method is used for

all but the initial 10-min step of each 6-hr integration cycle. The initial step in each integration cycle involves a Euler-backward step that possesses more desirable stability properties than does a forward step. The use of Euler-backward initial steps at the 6-hr restarting maintains the desired stability and greatly reduces solution separation.

c. Terrain, Truncation Error

A relatively realistic specification of the underlying terrain is used at FNWC. Early development runs have indicated the sensitivity of the model to variations in the height and character of the terrain. As a consequence, a more detailed terrain set based on values at 10-min latitude-longitude intersections is being completed by Leo Clarke of FNWC for use in an 89×89 fine-mesh model that will be programmed later this year.

Since more realistic terrain has been used, a type of modification was made in the pressure-force terms mentioned by Kurihara (1968) to reduce the inconsistent truncation error (and the resulting stationary noise patterns over high, irregular terrain). Instead of evaluating both the gradient of the geopotential distribution on a sigma surface and the terrain pressure gradient (invariant with altitude) as would be required by eq (1) and (2), the value of the geopotential is interpolated at neighboring gridpoint locations to the same pressure surface as at the computation point to enable one to compute the geopotential gradients on pressure surfaces which are thus synthesized locally around each computational point. As Kurihara notes, this does not solve the problem completely. Indeed, it was found that, for runs with this model in excess of 24 hr, addition of lateral diffusion was necessary to control the noise over and near the high terrain.

d. Lateral Diffusion

Lateral diffusion is applied to redistribute the unwanted small spatial scales in both the mass and motion fields, regardless of their origin. If diffusion operators are applied to sigma-surface temperatures directly, systematic warming results from the numerical procedure over mountain tops (ridges) with the opposite taking place in valleys. The same type of unrealistic redistributions of winds occur to a lesser extent, but in regions characterized by strong vertical wind shear the effect is both detectable and deleterious.

To avoid this difficulty, we applied the lateral diffusion on fields of the differences between the $(n-1)$th time-level values of the variables and their initial values. These difference fields are on the sigma surfaces. This method was found quite satisfactory. It bypasses the complicated forms for pressure-surface Laplacian operators transformed to sigma surfaces by the normal coordinate transformation rules.

e. Boundary Conditions

Two types of lateral boundary conditions have been tested in the past 2 yr at FNWC. The first to be used with some success was cyclic continuity on all boundaries. This means simply that cyclic continuity was imposed between the right and left boundaries and also between the upper and lower boundaries of the 59×59 point domain. This boundary condition was computationally stable for the longest term integrations made, but required flattening and blending of tropical regions at initialization time. In general, the adjustment processes in the lower latitudes were altered by this restructuring technique, and sometimes led to poor forecasts in the region from 40°N and southward.

The second type of boundary condition was the restoration technique described below. A field of restoration coefficients, k, that vary continuously (e.g., as a function of sine of latitude) from unity (at and south of 4°N) to zero (at and north of 17°N) is computed and saved. At the end of each 10-min time step, the new values (just obtained) of all forecast variables are restored back toward their values at the previous time step (in the region south of 17° N) according to the amount specified by the field of restoration coefficients.

For example, if the variable $u\pi$ has just been stepped forward by eq (12) in appendix 1, we would have at the $(n+1)$th time step (denoted by asterisk) the normally computed value for $u\pi$. This value is then modified by

$$u\pi^{(n+1)}=(1-k)u\pi_*{}^{(n+1)}+(k)u\pi^{(n-1)}. \qquad (7)$$

If $k=0$, clearly the value for $u\pi$ will not be altered. If $k=1$, it will be set back to its value at the $(n-1)$th time step. For values of k between 0 and 1, partial restoration is effected. The net effect is to produce a fully dynamic forecast north of 17°N, a persistence forecast south of 4°N, and a blend in between. The mathematical-physical effect of the technique is that the blend region acts as an energy "sponge" for outwardly propagating inertio-gravity oscillations. The initial fluxes on the grid-square boundary are preserved. No restructuring of the Tropics is necessary. These boundaries have been used routinely for integrations to 3 days with no perceptible difficulties in the products.

f. Initialization Procedures

For basic inputs to the model, we use the virtual temperature analyses for the Northern Hemisphere at 12 constant-pressure levels distributed from 1000 to 50 mb, height analyses at seven of these levels, and moisture analyses at four levels from the surface to 500 mb. In addition, we use a terrain field and sea-level pressure and sea-surface temperature analyses. Monthly mean surface temperature fields are used at present to derive an albedo field (Dickson and Posey 1967).

The initial nondivergent wind components are obtained from the stream function field, ψ, obtained by solution of a linear balance equation on pressure surfaces [eq (8)], with interpolation to sigma surfaces. These appear to be satisfactory for 2- to 3-day predictions. The equation is similar to the full balance equation, but the nonlinear term is evaluated using the geostrophic assumption;

that is,

$$2J(u_g, v_g)+f\nabla^2\psi+\nabla f \cdot \nabla\psi=\nabla^2\phi \quad (8)$$

where $J(u_g, v_g)$ is the Jacobian of the geostrophic wind components.

Plans are underway to shift to an iterative procedure for initializing the model following the guidelines of Winninghoff (1968). Although Winninghoff found that an iteration period equivalent to a 36-hr forecast might be necessary to effectively "adjust" the model, some type of compromise might be possible. That is, one might iterate only until such time as a reasonable set of dry omegas is generated.

g. Surface Stress

Frictional dissipation is accounted for in the gross boundary layer ($\sigma=1.0$–0.8) only. The stress is assumed to vanish at the top of this layer. The stress terms are the same as those used by Shuman and Hovermale (1968). The drag coefficient ($C_D=0.0015$) is, for the present, taken to be a constant. The surface wind speeds are obtained by extrapolation from neighboring sigma surfaces.

3. HEATING EFFECTS AND MOISTURE

The heating functions used in the model represent, in some measure, both an adaptation and extension of the work of Mintz and Arakawa as reported by Langlois and Kwok (1969). Terms representing evaporation and condensation processes, sensible heat exchange, solar and terrestrial radiation, and an Arakawa et al. (1969) parameterization of cumulus convection and precipitation are incorporated.

For the radiation terms, a gross albedo distribution determined as a function of the mean monthly surface temperature based on the work of Dickson and Posey (1967) is used. Smagorinsky's (1960) parameterization of "middle" cloudiness is used in the gross layer between $\sigma=0.8$ and 0.4 based on the forecast relative humidity.

Radiation, sensible heating, and evaporation are computed once each hour. Condensation, both large scale and cumulus type, is considered at each time step. Both moisture and heat are redistributed for the lower three layers in the Arakawa cumulus parameterization. Dry convective adjustment is performed at the conclusion of each step. Brief discussions of each of these physical processes and the methods by which they are evaluated numerically are given in the next few sections. Appendix 2 contains the very detailed quantitative description for these processes that is used in the model.

a. Radiation Processes

Radiative fluxes, both solar and terrestrial, are computed at levels where $\sigma=1.0$, 0.6, and 0.2, with flux divergences (and heating rates) then being calculated for the two gross layers thus defined. Temperature changes appropriate to the lower of these two gross heating layers are assigned arbitrarily to the model levels where $\sigma=0.9$ and 0.7. The temperature changes appropriate to the uppermost gross layer are assigned to the levels where $\sigma=0.5$, 0.3, and 0.1.

Solar radiation is modeled using the Mintz and Arakawa approach as developed by Joseph (1966). Both the insolation, S, at the top of the atmosphere and the precipitable water in the column are computed. S is assumed to be in two parts; $0.349S$, which is subject to absorption and reflection but not scattering, and $0.651S$, which is subject to scattering but not absorption. After considering the degree of middle cloudiness, one calculates the heating rates by making the additional assumptions that (1) in-cloud path length is 1.66 the normal length, (2) an arbitrary amount of water vapor is added to account for the presence of clouds, (3) the reflected radiation for cloud tops is subject to absorption only, and (4) the cloud albedo is 0.5. Finally, the solar radiation reaching the ground (to be used later in the calculation of sensible heat and evaporation) is determined.

In the long-wave radiation computations, the method of Danard (1969) is followed initially using Kuhn's data (1963) for water vapor emissivities and assuming that the ground temperature is given by an extrapolated temperature from the levels $\sigma=0.9$ and 0.7. Then the technique given by Langlois and Kwok (1969) is used to correct these flux computations using analyzed sea-surface temperature or temperatures obtained by solution of a heat balance equation over land areas when the sensible heating is computed. As before, the middle cloudiness amount is used to apportion the rates for the clear and overcast conditions.

b. Sensible Heat and Evaporation

Sensible heating is determined as a function of the air temperature–surface temperature difference and may lead to some difficulties because we do not predict temperatures, winds, and moistures sufficiently close to the surface. Evaporation over water is computed as a function of the saturation moisture at the surface and the moisture near the surface. To overcome this difficulty, we assume the air near the surface to be a very thin boundary layer that does not absorb or store a significant amount of heat or moisture. The fluxes of moisture and heat, therefore, are the same through the top and bottom of this thin layer.

Evaporation over land is calculated from a Bowen ratio, using data from Budyko as given in Sellers (1965).

Surface temperatures are given as indicated in subsection 3a.

c. Condensation and Parameterized Convection

The total condensation occurring in the model is the sum of that resulting from two processes. The first of these, based on the empirical fact that the atmosphere is not supersaturated to any significant degree, results from large-scale advection and is merely the application of the constraint of 100-percent relative humidity. The second process, based on averaged stability characteristics of the atmosphere, results from the parameterization of cumulus-scale convection recommended by Arakawa.

Advective-scale condensation. The release of latent heat and the amount of moisture change are based on an economical solution procedure given by Langlois and Kwok (1969) to the equation

$$c_p(T_{\text{new}}-T_{\text{old}})=L(q_{\text{old}}-q_{\text{new}}) \tag{9}$$

where q is the moisture variable, c_p is the specific heat at constant pressure, and L is the latent heat.

If supersaturation exists at the lowest computational level, then the excess is precipitated. At the same time, the temperature will rise (from T_{old} to T_{new}). This process is modified slightly at higher levels by checking the possibility of evaporating precipitated water into the next lower level and letting rain fall to the ground only if that next lower level either was or became saturated.

Parameterized convection. Three types of convection are considered: high cumulus (involving levels where $\sigma=0.5$, 0.7), deep penetrating convection (involving levels where $\sigma=0.9$, 0.7, 0.5), and low cumulus (involving levels where $\sigma=0.9$, 0.7). Precipitation may result from the first two types. Two energy parameters,

$$h=c_pT+gz+Lq \tag{10}$$

and

$$E_n=c_pT+gz+Lq_s, \tag{11}$$

are used in conjunction with measures of the total upward convective mass flux, as well as the entrainment, to determine the degree of conditional instability of the column. The term q_s represents saturation specific humidity. Note that E_n is constant along a moist pseudoadiabat, and the difference $(h-Lq)$ is constant along a dry adiabat.

4. FOUR-PROCESSOR PARTITIONED MODEL

During the period frcm May until August 1970, the FNWC primitive-equation model was programmed to run in a four-processor mode using two dual-processor CDC 6500 computers. To accomplish this, we required answers to three different types of questions:

1. How should the computational segments of the system of difference equations be partitioned into four approximately equal segments?
2. How should the standard CDC 6500 operating system be modified to enable four programs on two computers to communicate with each other via extended core, while at the same time preventing other programs from interfering?
3. How should an efficient and foolproof program synchronization mechanism be designed to ensure that all four programs start and remain in correct time phase?

It is beyond the scope of this paper to treat questions 2 and 3. These are covered in considerable detail in a paper by Beckett et al. (1971). The following discussion will describe the way in which the computational load was partitioned to permit four-way parallel execution of the programs.

The problem was divided into three main categories: the initialization section, the typical time step, and the output section.

In the input/initialization section, the computational burden was split three ways; processors 2 and 3 each solve the balance equation on one-half of the required pressure surfaces (from 1000 to 50 mb) while processor 1 initializes everything else (temperatures, terrain pressure, moisture, etc.).

In a typical time step, a three-way split is accomplished first, and then a four-way split takes place. First, consider the three-way split. Processor 1 integrates the continuity equation to obtain the local change in terrain pressure, and the vertical-velocity fields at the layer interfaces. Processor 2 computes the geopotential field correction terms for the five computational levels (for the y-direction momentum equation, Kurihara modification), while processor 3 computes these same five geopotential correction fields for the x-direction momentum equation. Secondly, a four-way split is possible once the aforementioned fields are available. In processor 1, the y-direction momentum equation is integrated at five levels. The x-direction momentum equation is integrated in processor 2 at five levels. The thermodynamic energy equation is put into processor 3 to obtain the five new levels of temperatures. Integrating the moisture continuity equation yields three new levels of moistures in processor 4. Interspersed with the three levels of moistures in processor 4 is the routine for large-scale condensation, the evaporation of this precipitation into layers beneath (where appropriate), and the associated temperature changes. To do this in proper time phase, we need an intrastep second level of synchronization between processors 3 and 4. Because processor 4 handles only three levels of moistures, and because the first three levels of new temperatures are available concurrently with the three levels of moistures, it is possible for processor 4 to commence the cumulus parameterization routine while processors 1, 2, and 3 are working on their assignments at level 4. At the conclusion of the fifth level of temperatures (and at very nearly the same instant that the cumulus parameterization is completed), the dry convective adjustment (involving five levels of new temperatures) routine is started in processor 4. When the final temperature distributions are available from this routine, the new geopotential fields are computed in processor 4 by integrating the hydrostatic equation.

A three-way partition is effected in the *output section* (which is entered every 6 hr during the forecast period). Processor 1 outputs those 54 fields (mostly on sigma surfaces) required to restart the model from any output time if necessary. Processors 3 and 4 process the output fields (transformation of coordinates, fill in values under terrain, filter) and output about 58 data fields each output time to the disk or tape.

Once each six time steps, the so-called "heating package" is evaluated. This results in a three-way partition of the computational segments pertaining to solar radiative and terrestrial radiative fluxes, evaporation from the underlying surface, and sensible heat exchange. These segments go in processors 1, 2, and 3 just after the new winds and temperatures are completed for level 5 but

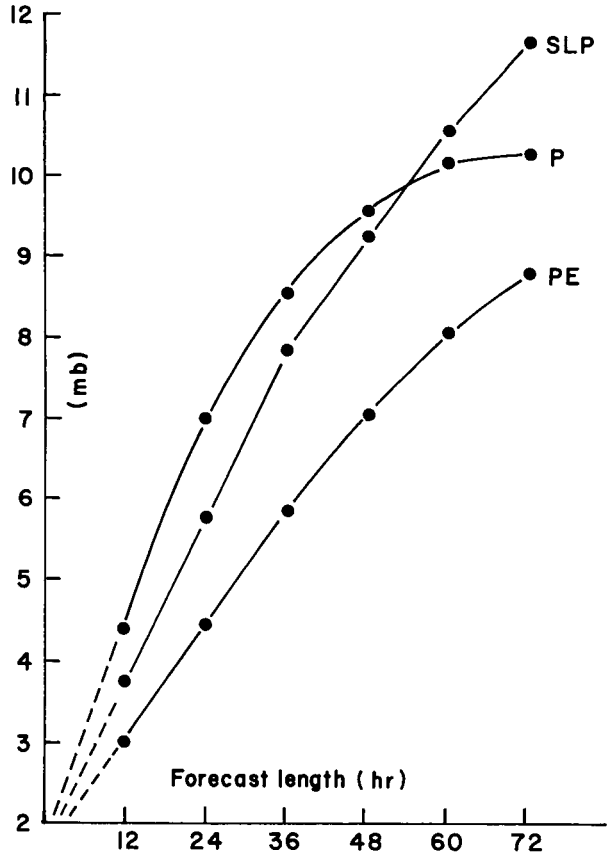

FIGURE 2.—Verification statistics (mean rms errors) for forecasts of sea-level pressure for November 1970–January 1971. Curve SLP refers to the forecast by the previous barotropic-thickness advection model. Curve P refers to a persistence forecast. Curve PE refers to the forecast by the primitive-equation model.

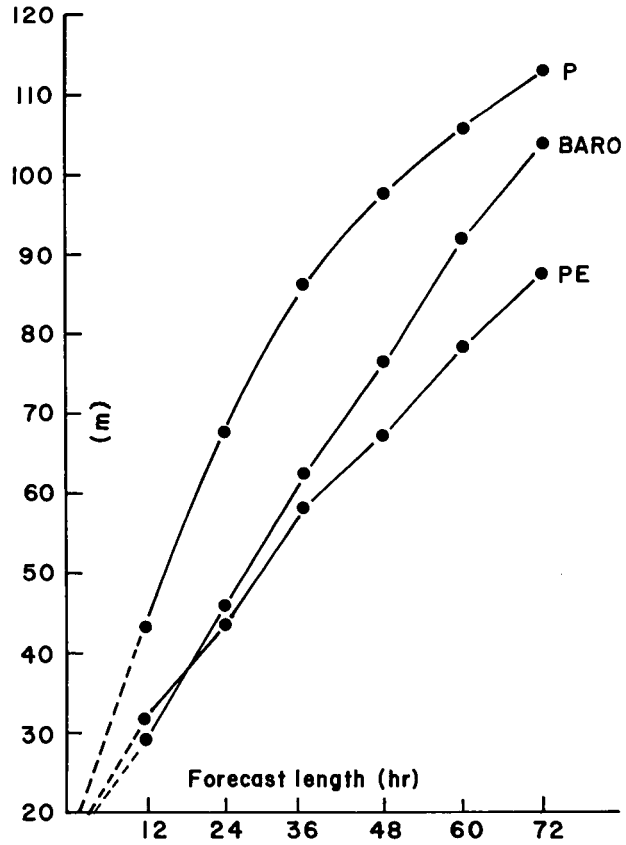

FIGURE 3.—Verification statistics (mean rms errors) for forecasts of 500-mb height for November 1970–January 1971. Curve BARO refers to the forecast by the previous barotropic-thickness advection model. Curve P refers to a persistence forecast. Curve PE refers to the forecast by the primitive-equation model.

before the dry convective adjustment routine is started in processor 4.

5. RESULTS

The application of the primitive-equation (PE) model to numerical weather prediction during 1970 and 1971 led to an unqualified improvement in the capability at FNWC, particularly in the winter half of the year. Figures 2 and 3 compare results of the PE model and FNWCs previous operational model for November 1970, December 1970, and January 1971.

The earlier model was based on a quasi-geostrophic divergent barotropic model modified empirically to take into account effects of mountains, baroclinicity, and large-scale sensible heating at the 500-mb level. Added to this was an empirically adjusted thickness advection scheme to forecast the sea-level pressure. The products of this model are referred to as "BARO" and "SLP," respectively, in the figures. The persistence error curve is denoted by "P" and the PE-model error is so marked. All values are in terms of root-mean-square (rms), in millibars and meters with the verifications taken over the Northern Hemisphere north of 20°N. In general, the PE surface prognostics are about four times as skillful at 36 hr as the SLP using this measure of skill. Notable is the relative increase in the skill of the PE model over the SLP with time. This feature is also present for the upper level prognoses although the margin of difference is not so great.

In summer on the other hand, rms scores are nearly the same for the SLP and PE model at 36 hr over the entire hemisphere. In fact, surface scores then appear similar to the upper level scores of figure 3. Upper level scores in summer actually tend to be slightly better for the BARO to about 36 hr. Qualitatively, however, there is so much more valuable information that can be produced objectively by the PE model (i.e., forecasts of vertical temperature and wind profiles, moisture and precipitation, derived surface winds) that confining oneself merely to comparisons of rms error scores for surface pressure or 500-mb height may be seriously misleading in judging a model's true capability in serving as a source of guidance material for actual weather forcasting.

In addition to reproducing the essential features of the verification analyses both at sea level and at 500 mb, the model shows considerable promise in its ability to simulate the growth of baroclinic disturbances. This is particularly evident in the western Pacific Ocean in winter where many storms in the winters of 1969–70 and 1970–71 were predicted.

A very interesting case of cyclogenesis occurred on Jan. 30–31, 1970, in the western Pacific. In 36 hr, a low-

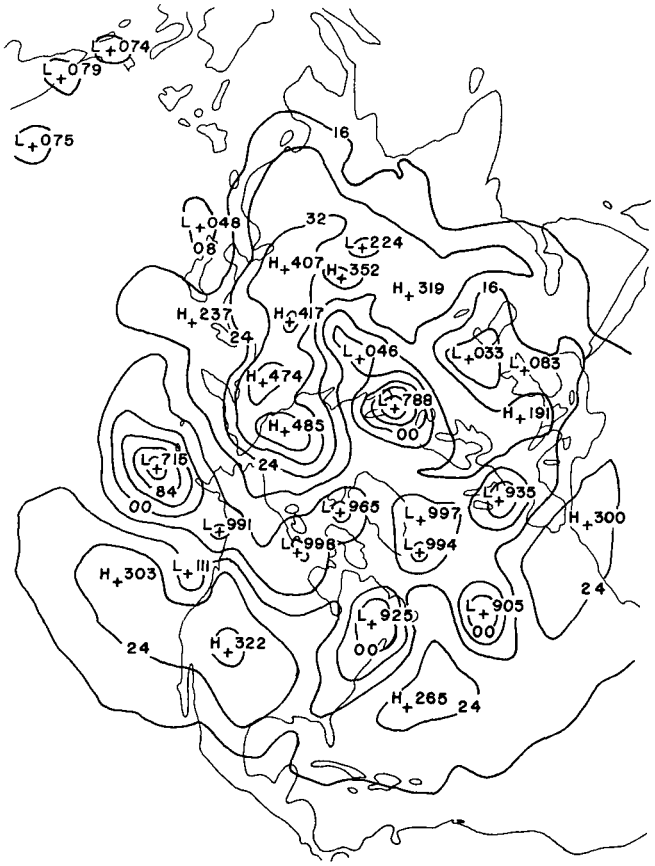

FIGURE 4.—Initial sea-level pressure analysis at 0000 GMT, Jan. 30, 1970.

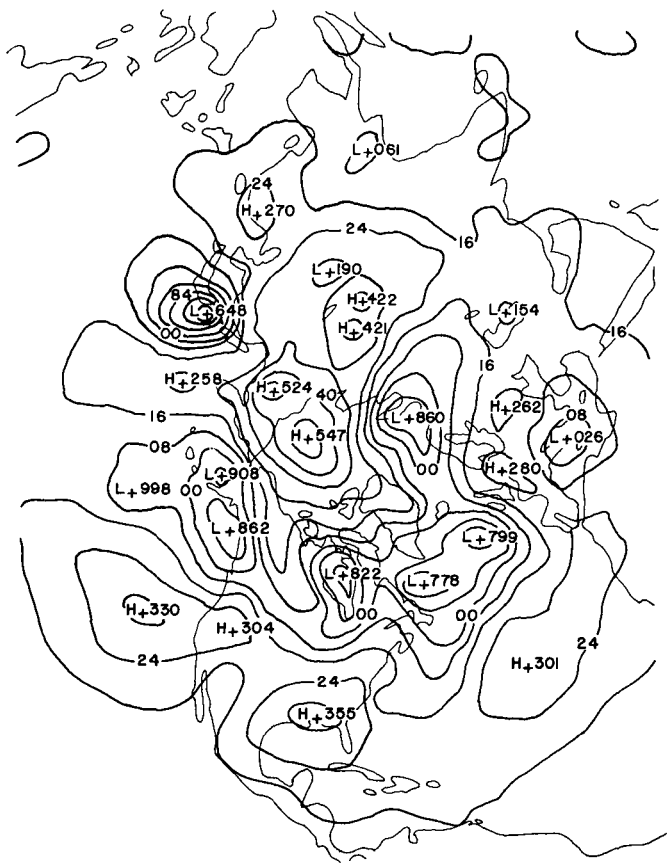

FIGURE 5.—Verification for the sea-level pressure analysis at 1200 GMT, Jan. 31, 1970.

pressure center south of Japan deepened from 1005 to 965 mb. Several runs of the model were made at this time in which one feature at a time was varied to illustrate the effects on this one cyclone in particular. Figures 4–10 show the outcome. Figures 4 and 5 contain the initial and verification sea-level analyses from FNWC. Figure 6 shows the 36-hr prognosis from the version of the model in which heating terms and a relatively smooth terrain are present, restoration boundaries are used, and the initial winds are specified by the linear balance equation. Note that the storm deepened to 961 mb, an excellent forecast. In figure 7, the 36-hr forecast for the storm is shown from a model which is the same as that in figure 6 except that cyclic lateral boundary conditions are used. Although considerable alteration of initial fields was involved south of 23°N, there is no significant effect on the cyclone. In figure 8, on the other hand, the version of the model is the same as in figure 6, but the initial winds are specified from the geostrophic equation with a constant Coriolis parameter (0.0001). Here, the cyclone deepened to only 981 mb. In figure 9, the version of the model is again the same as in figure 6 except that the heating terms are not present. The cyclone deepened to only 991 mb or nearly the same (994 mb) as the SLP model (not shown). Finally, figure 10 shows the hemispheric forecast from our present operational version of the model. Here, we have replaced the relatively smooth terrain with more realistic terrain.

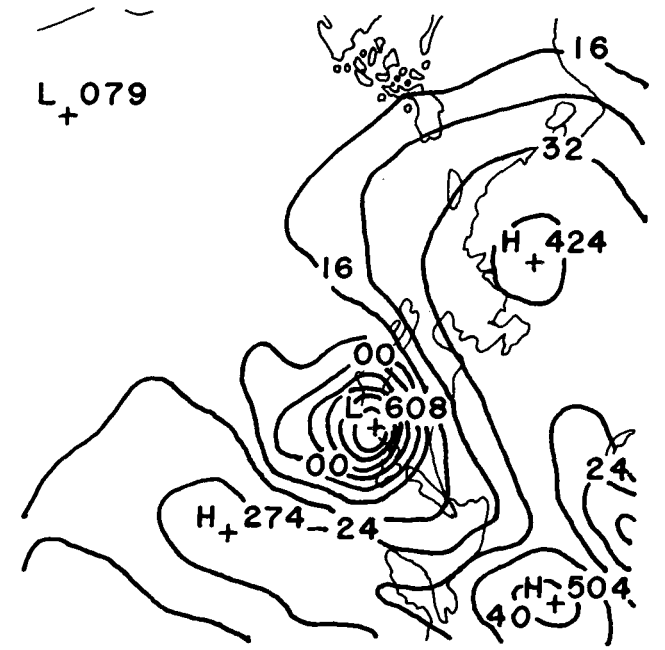

FIGURE 6.—Forecast using smoother terrain, total heating, linear balanced initial wind, and restoration procedure on the boundaries.

However, the effect on the maritime cyclone was small. It deepened to 962 mb.

It is apparent from these figures that the heating was of greatest importance for forecasting this case of cyclogenesis, but it is also apparent that varying the initial

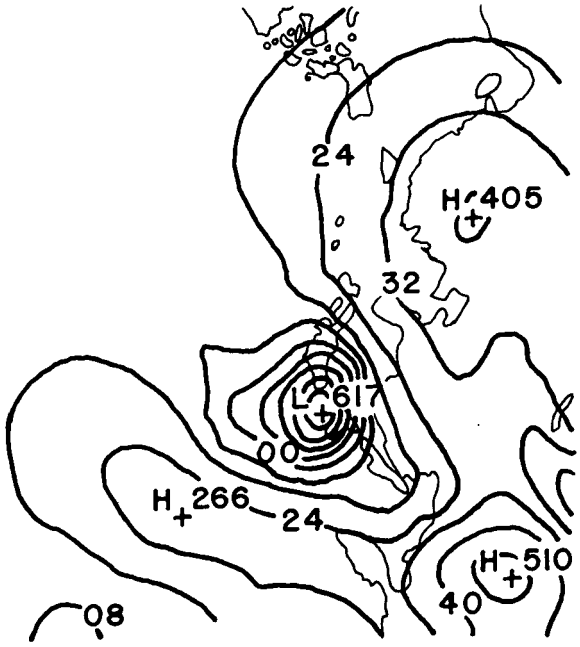

FIGURE 7.—Same as figure 6 except the cyclic lateral boundary condition is used.

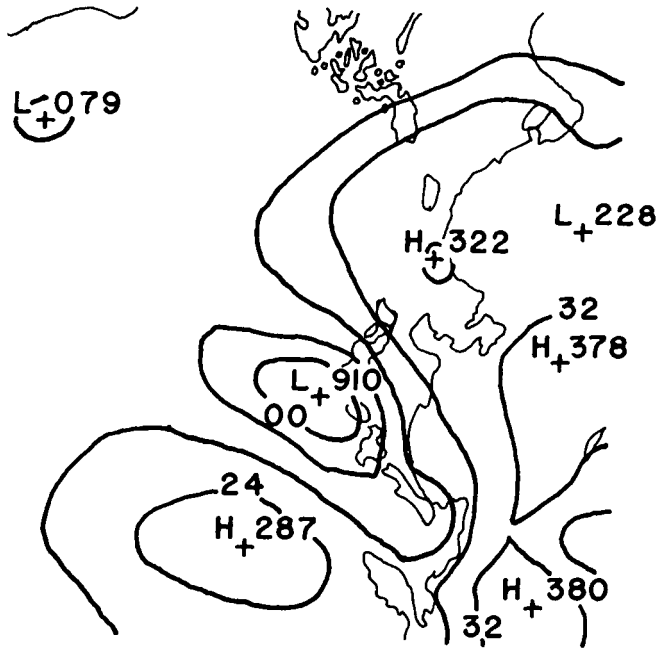

FIGURE 9.—Same as figure 6 except the heating is eliminated.

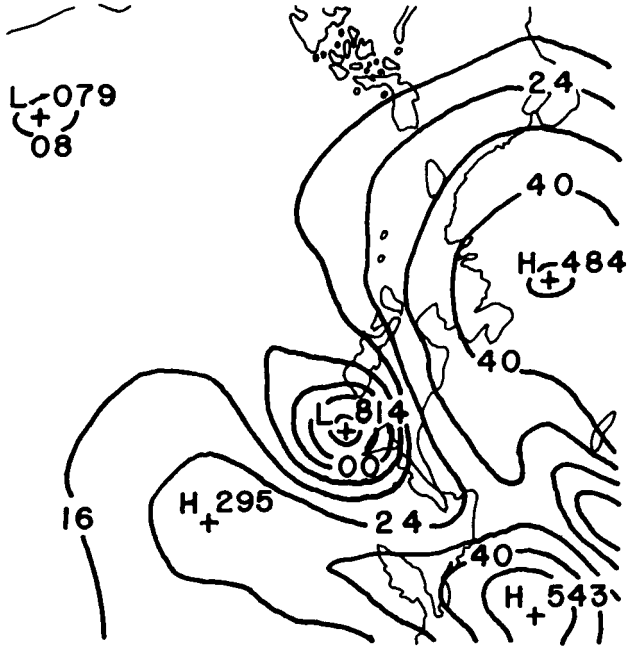

FIGURE 8.—Same as figure 6 except the geostrophic initial wind ($f=0.0001$) is used.

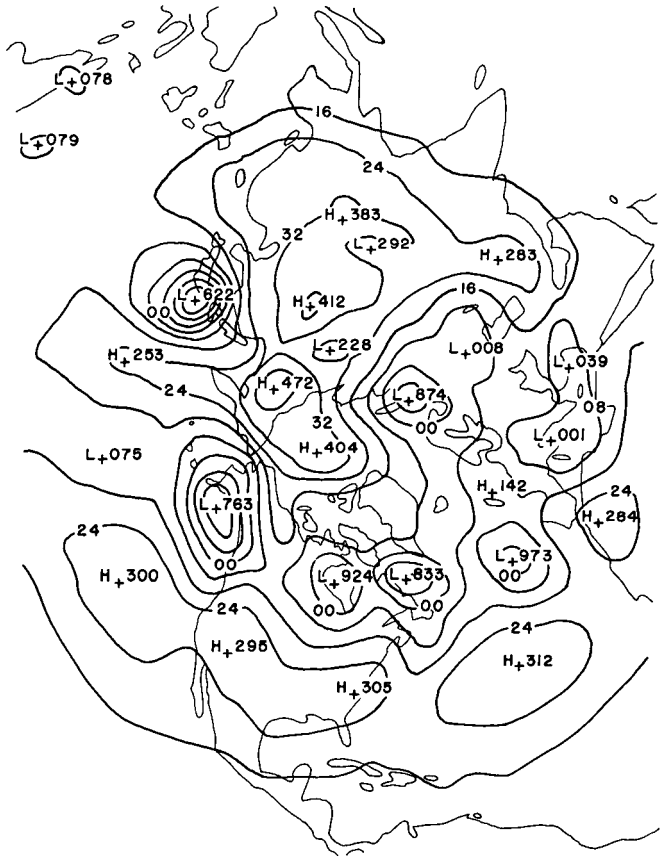

FIGURE 10.—Same as figure 6 except a more realistic terrain is used.

specification of the wind has an important effect. Boundary conditions, as long as they were reasonable, or some variation of the terrain are not so important for this case.

The information contained in this map set constitutes a very interesting but by no means complete treatment for this type of event. The set is an indication of the vast potential and at the same time of the sensitivity of the PE model and emphasizes the need for a careful specification of all effects for the best result. By showing the admittedly exceptional case, there is no intention to minimize the normal sources of error; that is, truncation error, initialization error, and errors resulting from the statistical formulation of heating and friction. Analysis for each of these is beyond the scope of this paper. Fur-

thermore, with real data, where the effects of the several error sources are always mixed in an unknown manner, such analyses would be impossible.

6. FUTURE DEVELOPMENT

The areas for improvement in which real hope exists appear to be related to the reduction of truncation error by shifting to a finer mesh and to the reduction of initialization error by improvements in the data base or analysis scheme. Other improvements of a more minor nature will no doubt result from refinements in numerical techniques or in the improved formulation of specific terms (such as the heating functions).

There are several aspects to the initialization problem. These include, but are not limited to, the number, distribution, type, and quality of observations and to the manner in which these observations are employed to model the state parameter structure. Although the number of observations constitutes an acute problem, it is not a present pursuit for the authors. We are hopeful, though, that soundings from satellites will be available in large numbers in the coming years. Rather, our efforts will be concentrated on analysis models that *dynamically condition* the state parameter structure and on techniques that derive from these structures the initial wind distributions and the like. Because our experience level with baroclinic primitive-equation models is still limited, we need to examine the implied phase relationships to determine which perturbations, real or fictitious, lead to baroclinic developments. Also, we need to know if perturbations can be eliminated through quality control from the initial analyses.

As to the matter of truncation error, one can fall back on recognizable constraints. How much time can be taken to produce a 3-day forecast? How many points can be in the grid? How many levels? Is the computer power available to do the type of job that is required? Looking into the very early 1970s, it appears that prediction will be possible on an 8,000-point grid rather than on our current 4,000-point grid. For the immediate future, the five-layer resolution in the vertical is reasonable. In addition, those computational segments for which the physics is reasonably firm can be coded in machine language. At the current time, 100 percent of our CDC 6500 computer capability and 50 percent of our extended core capacity is used. Shifting to an 8,000-point grid would ordinarily require additional central memory, necessitating a different approach to partitioning the model. For this version, a plan to partition the horizontal domain into fourths (instead of the computational burden) is being formulated. This will actually cut the central memory requirement by 15 percent because one-fourth of the points in fields twice their current size will be used. Further, the scheme will allow a 72-hr prognosis to be executed in 4 hr instead of the 5 hr and 20 min required by the current partitioning scheme.

Ultimately, the operational model must be extended to the global domain and formulated for the ocean-atmosphere system to extend its range of predictability. With the development of the next generation of computers, these projects will become feasible.

APPENDIX 1: THE FINITE-DIFFERENCE EQUATIONS

The momentum equation in the x-direction is given by

$$(\pi u)_*^{n+1}=(\pi u)_*^{n-1}+2\Delta t\left\{\left[-\mathcal{L}(u)_*+f(\pi_* v_*)-\left(\frac{\Delta\phi}{\Delta x}\right)_*\right]^n-F_x^{n-1}+K\frac{m_{i,j}^2}{d^2}(\nabla^2 D_u)_*^{n-1}\right\} \quad (12)$$

and in the y-direction by

$$(\pi v)_*^{n-1}=(\pi v)_*^{n-1}+2\Delta t\left\{\left[-\mathcal{L}(v)_*-f(\pi_* u_*)-\left(\frac{\Delta\phi}{\Delta y}\right)_*\right]^n-F_y^{n-1}+K\frac{m_{i,j}^2}{d^2}(\nabla^2 D_v)_*^{n-1}\right\} \quad (13)$$

where the subscript $(*)$ denotes the point (i,j,k), the superscripts denote the time level, $\mathcal{L}$ is the finite-difference advective operator defined in eq (19), ∇ is the centered time and space difference operator, and ∇^2 is the finite-difference Laplacian defined in eq (19). Other symbols are as used in subsection 2a of the text except that here the difference fields explained in subsection 2d are denoted explicity as D_u and D_v with K being the lateral diffusion coefficient; $m_{i,j}$ is the map factor, d is the grid mesh size and Δt is the time step. The $(n-1)$ notation on the diffusion terms refers to the time level of one of the fields forming the difference field.

The lower boundary pressure is computed from

$$\pi_{i,j}^{n+1}=\pi_{i,j}^{n-1}+2\Delta t\left(\frac{\partial\pi}{\partial t}\right)_{i,j}^n \quad (14)$$

where, for the entire column, one evaluates the local change as

$$\left(\frac{\partial\pi}{\partial t}\right)_{i,j}^n=-\sum_{k=1}^{5}0.1\frac{m_{i,j}^2}{d}(\alpha_{i+1,j,k}-\alpha_{i-1,j,k}+\beta_{i,j+1,k}-\beta_{i,j-1,k})^n \quad (15)$$

where, for notational convenience, we define the quantities

$$\alpha\equiv\frac{u\pi}{m} \quad (16)$$

and

$$\beta\equiv\frac{v\pi}{m}. \quad (17)$$

The thermodynamic equation takes on the form

$$(\pi T)_*^{n+1}=(\pi T)_*^{n-1}+2\Delta t\left\{-\mathcal{L}(T)_*+\frac{RT_*}{\sigma_k c_p}\left[-\frac{\pi_{i,j}}{2}(w_k+w_{k-1})_{i,j}+\sigma_k\left(\frac{\partial\pi}{\partial t}\right)_{i,j}+\frac{\sigma_k m_{i,j}}{2d}(\mathbf{V}_*\cdot\nabla\pi)\right]^n+\frac{Km_{i,j}^2}{d^2}\nabla^2(D_T)_*^{n-1}+H_*\pi_{i,j}^{n-1}\right\} \quad (18)$$

with $w\equiv-d\sigma/dt$, the vertical motion.

The advective operator and the Laplacian are defined as

$$\mathcal{L}(\psi)_*\equiv\frac{m_{i,j}^2}{4d}\{[(\alpha_{i+1}+\alpha_i)(\psi_{i+1}+\psi_i)-(\alpha_{i-1}+\alpha_i)(\psi_{i-1}+\psi_i)]_{j,k}$$
$$+[(\beta_{j+1}+\beta_j)(\psi_{j+1}+\psi_j)-(\beta_{j-1}+\beta_j)(\psi_{j-1}+\psi_j)]_{i,k}\}$$
$$+\frac{\pi_{i,j}}{0.4}[w_k(\psi_{k+1}+\psi_k)-w_{k-1}(\psi_k+\psi_{k-1})]_{i,j} \quad (19a)$$

$$\nabla^2(\psi)_*\equiv(\psi_{i+1,j}+\psi_{i-1,j}+\psi_{i,j+1}+\psi_{i,j-1}-4\psi_{i,j}). \quad (19b)$$

Vertical motions for nonmaterial surfaces are obtained from a form of the continuity equation

$$w_{i,j,k+1}=w_*-\frac{0.2}{\pi_{i,j}}\left\{\left(\frac{\partial\pi}{\partial t}\right)_{i,j}+\frac{m_{i,j}^2}{2d}[(\alpha_{i+1}-\alpha_{i-1})_{j,k}+(\beta_{j+1}-\beta_{j-1})_{i,k}]\right\} \quad (20)$$

The hydrostatic equation is given at the lowest level by

$$\phi_*-\phi_{\text{Terrain}}-RT_*\ln(0.9) \quad (21)$$

and, for subsequent levels,

$$\phi_{k+1}=\phi_k-R\ln\left(\frac{\sigma_{k+1}}{\sigma_k}\right)\left[\frac{T_k\ln\left(\frac{\sigma_k}{\pi}\right)+T_{k+1}\ln\left(\frac{\sigma_{k+1}}{\pi}\right)}{\ln\sigma_k+\ln\sigma_{k+1}-2\ln\pi}\right]. \quad (22)$$

Finally, the moisture equation is given by

$$(\pi q)_*^{n+1}=(\pi q)_*^{n-1}+2\Delta t\left[-\mathcal{L}(q)_*^n+Q_*\pi_{i,j}^{n-1}+K\frac{m_{i,j}^2}{d^2}\nabla^2(D_q)_*^{n-1}\right]. \quad (23)$$

In eq (12) and (13), the pressure gradient terms are evaluated in the special manner near high terrain indicated in subsection 2c.

APPENDIX 2: HEATING AND MOISTURE SOURCE TERMS

The heating functions are formulated following closely the approach used by Mintz and Arakawa as outlined by Langlois and Kwok (1969). Formally, the heating can be written

$$H=H_{sw}+H_{Lw}+H_c+H_\Gamma \quad (24)$$

where H_{sw} refers to the heating due to absorption of short-wave solar radiation; H_{Lw}, the heating due to absorption of terrestrial infrared radiation; H_c, the heating resulting from the condensation of water vapor; and H_Γ, the heating due to sensible heat transfer from the surface.

Solar Radiation

The incoming solar radiation at the top of the model atmosphere is given by

$$S=S_0\cos\mu \quad (25)$$

where S_0 is the solar constant and μ is a function of time of day, latitude, and season.

The heating of the atmosphere is dependent on the vertical distribution of moisture above each gridpoint. The scheme constructed by Joseph (1966) and explained in subsection 3a is followed. For the radiation calculations, the model carries a simple form of middle cloud which is assumed to exist between $\sigma=0.4$ and 0.8. Use of Smagorinsky's (1960) empirical formula for middle clouds,

$$CL=2.0\left(\frac{e}{e_s}\right)_{0.7}-0.7, \quad (26)$$

gives the amount of cloudiness, CL, in terms of the relative humidity at $\sigma=0.7$. Limits of 1.0 and 0.0 are set on the range of values given from eq (26). Here, e is vapor pressure and e_s is saturation vapor pressure.

The absorption of incoming solar radiation for the upper layer ($\sigma=0$ to $\sigma=0.6$) is given by

$$A_2=[(1-CL)\mathcal{J}_1+CL(1-\alpha_c)\mathcal{J}_2]0.349S \quad (27)$$

and for the lower layer ($\sigma=0.6$ to $\sigma=1.0$) by

$$A_1=[(1-CL)\mathcal{J}_3+CL(1-\alpha_c)\mathcal{J}_4]0.349S \quad (28)$$

where

$$\mathcal{J}_1=0.271\left[pw(3)\frac{S_0}{S}\right]^{0.303}, \quad (29)$$

$$\mathcal{J}_2=0.271\left\{1.66\left[\frac{pw(c)}{2}+pw(3)\right]\right\}^{0.303}, \quad (30)$$

$$\mathcal{J}_3=0.271\left\{\left[pw(3)+pw(2)+pw(1)\right]\frac{S_0}{S}\right\}^{0.303}-\mathcal{J}_1, \quad (31)$$

and

$$\mathcal{J}_4=0.271\left\{1.66\left[pw(c)+pw(3)+pw(2)+pw(1)\right]\right\}^{0.303}-\mathcal{J}_2, \quad (32)$$

and where pw is the precipitable water given by

$$pw=\frac{1}{g}\int_0^p 0.622\frac{e}{1000}\,dp. \quad (33)$$

The amount of liquid water assumed to be present in the cloud, $pw(c)$, is arbitrarily set at 4 g·cm^{-2}.

These absorption functions are from Manabe and Möller (1961). The cloud's albedo, α_c, is set at 0.5. Finally, the amount of solar radiation that reaches the surface, S_g, is needed because this will be used in the calculation of sensible heating over the land areas. Following Mintz and Arakawa,

$$S_g=(1-\alpha_g)\left((1-CL)\left[0.349S-A_2-A_1+\frac{0.651S(1-\alpha_S)}{1-\alpha_S\alpha_g}\right]+CL\left\{\frac{0.349S[(1-\alpha_S)-(1-\alpha_c)(\mathcal{J}_1+\mathcal{J}_2)]}{1-\alpha_c\alpha_g}+\frac{1-\alpha_{Sc}}{1-\alpha_{Sc}\alpha_g}0.651S\right\}\right). \quad (34)$$

In eq (34), α_g, the ground surface albedo, is given as a function of latitude over the sea and as a function of snow cover over the land, α_S is albedo of clear sky, and α_{Sc} is the albedo of cloudy sky. The snow cover is assumed to be a function of mean monthly temperature.

Terrestrial Radiation

The infrared fluxes at $\sigma=1.0$, 0.6, and 0.2, are computed in the manner suggested by Mintz and Arakawa:

$$F_{1.0}=F^*_{1.0}+St(T_g^4-T_s^4), \tag{35}$$

$$F_{0.6}=F^*_{0.6}+\frac{0.8(1-CL)(F_{1.0}-F^*_{1.0})}{1+1.75[pw(1)+pw(2)]^{0.416}}, \tag{36}$$

and

$$F_{0.2}=F^*_{0.2}+\frac{0.8(1-CL)(F_{1.0}-F^*_{1.0})}{1+1.75[pw(1)+pw(2)+pw(3)]^{0.416}} \tag{37}$$

where St is the Stefan-Boltzmann constant.

$F^*_{1.0}$, $F^*_{0.6}$, and $F^*_{0.2}$ are the fluxes computed by assuming the surface temperature is given by a downward extrapolated temperature, T_s. The factor 0.8 is an empirical correction to account for the effect of CO_2.

In eq (35), T_g is given over the oceans by the operational sea-surface analyses; over the land areas it is given by the solution of a heat balance equation to be explained in the section on sensible heat transfer and evaporation.

To compute the approximate fluxes, F^*, we used the method developed by Danard (1969), with an emissivity function for water vapor from Kuhn (1963). Thus,

$$F^*_{1.0}=St((1-CL)\{-T_s^4+T_{0.8}^4\varphi(X1)+T_{0.3}^4[\varphi(X2)-\varphi(X1)]\}+CL[T_{0.8}^4-T_s^4+(T_{0.9}^4-T_{0.8}^4)\varphi(X4)]), \tag{38}$$

$$F^*_{0.6}=St\{(1-CL)[-T_s^4+(T_s^4-T_{0.8}^4)\varphi(X1)+T_{0.3}^4\varphi(X3)]\}, \tag{39}$$

and

$$F^*_{0.2}=St((1-CL)\{-T_s^4+(T_s^4-T_{0.8}^4)[\varphi(X2)-\varphi(X3)]+(T_s^4-T_{0.3}^4)\varphi(X3)\}+CL[-T_{0.4}^4]) \tag{40}$$

where

$$\varphi(XN)=0.0105(XN)^2+0.1675(XN)+0.542, \tag{41}$$

$$X1=\log_{10}[pw(1)+pw(2)], \tag{42}$$

$$X2=\log_{10}[pw(1)+pw(2)+pw(3)], \tag{43}$$

$$X3=\log_{10}[pw(3)], \tag{44}$$

and

$$X4=\log_{10}[pw(1)]. \tag{45}$$

For these calculations, pw (eq 33) is modified to

$$pw=\frac{1}{g}\int_0^p 0.622\,\frac{e}{p}\left(\frac{p}{1000}\right)^{0.85}\left(\frac{273}{T}\right)^{0.5}dp. \tag{46}$$

Finally, to convert to a heating rate we use

$$H_{Lw_e}=-(F_{1.0}-F_{0.6})\,\frac{9g}{\pi c_p}\ (°\text{C/hr}) \tag{47}$$

and

$$H_{Lw_l}=-F_{0.6}-F_{0.2})\,\frac{9g}{\pi c_p}\ (°\text{C/hr}) \tag{48}$$

because the fluxes are computed in cgs units.

Sensible Heating and Evaporation

Sensible heating is computed as a function of the difference of the surface temperature, T_g, and the temperature of the air near the surface, T_x. Similarly, evaporation is computed as a function of the saturation moisture at the surface, q_s, and the moisture near the surface, q_x. Difficulty arises in our model as near-surface temperature, wind, or moisture is not predicted. To surmount this difficulty, we followed the technique used by Mintz and Arakawa.

The air near the surface is assumed to be a very thin boundary layer which does not absorb or store a significant amount of heat or moisture. The fluxes of sensible heat and moisture are, therefore, the same through the top and the bottom of this thin boundary layer. Generally, for heat transfer an equation of the form

$$\Gamma=-K_H\frac{\Delta\theta}{\Delta z} \tag{49}$$

is used where θ is potential temperature. Equation (49) is modified by Mintz and Arakawa to

$$\Gamma=\rho_{1.0}c_p\frac{K^*}{\left[1+\frac{a^*(\theta_{0.9}-\theta_s)}{(z_{0.9}-z_{1.0})}\right]}\left[\gamma_c-\frac{(\theta_{0.9}-\theta_x)}{(z_{0.9}-z_{1.0})}\right]. \tag{50}$$

In eq (50), the expression for K_H is allowed to vary with the stability of the lowest level. K^*, a^*, and γ_c are empirical constants. The constant γ_c allows for a somewhat more realistic variation of Γ between day and night. The subscript s refers to the value of a parameter extrapolated to the surface from the levels $\sigma=0.9$ and 0.7.

The sensible heat flux through the bottom of the boundary layer is given by the equation

$$H_\Gamma=\rho_{1.0}c_pC_DV_s(T_g-T_x) \tag{51}$$

where for this computation

$$V_s=0.7|\mathbf{V}_s|+G_u \tag{52}$$

where G_u, the gustiness factor, is 2.2 m/s.

From eq (50) and (51), T_x can be obtained, given T_g. Over the land areas, T_g must be computed from a surface heat balance equation,

$$(1+r)H_\Gamma-S_g+F_{1.0}=0, \tag{53}$$

in which only the heat storage has been neglected. We have used data from Budyko (given in Sellers 1965) to determine r, a Bowen ratio,

$$r=9.6\ (\sin\phi)^2-7.93\ (\sin\phi)+2.0 \tag{54}$$

where a minimum value of 0.4 for $\sin\phi$ is enforced.

Equation (53) is modified over ice-covered ocean to

$$(1+r)H_\Gamma - S_g + F_{1.0} = B(T_w - T_g) \tag{55}$$

where B is an ice conduction coefficient and $T_w = 271.2°K$.

Evaporation over the ice-free ocean is determined in a similar manner to the heat flux. The equation resulting is

$$E = \frac{\rho_{1.0} c_p V_s}{1 + \frac{\pi c_p V_s}{10 g \rho_{1.0}} \left[\frac{K^*}{1 + \frac{a^*(\theta_{0\,9} - \theta_{0\,7})\pi}{10 g \rho_{1.0}}} \right]} (q_s - q_x) \tag{56}$$

with the approximate relation

$$q_s = \frac{0.622 e (AE - BE/T_g)}{\pi - e^{(AE - BE/T_g)}} \tag{57}$$

with $AE = 21.656$ and $BE = 5418$.

The details of the derivation of eq (56) are given by Langlois and Kwok (1969).

Heating Resulting From Condensation

The computed release of latent heat is based on the assumptions that, for synoptic scale motion, the atmosphere is not in a supersaturated state or it does not exceed a certain degree of conditional instability.

To satisfy the first of these, we must solve the equation (subsection 3c)

$$c_p(T_{\text{new}} - T_{\text{old}}) = L(q_{\text{old}} - q_{\text{new}}). \tag{58}$$

An approximate, but relatively economical, solution procedure is outlined by Langlois and Kwok (1969).

If the computation is for the lowest level of the model, and if supersaturation (q_{old}) occurs, then some amount of water must be condensed to reduce the amount of water vapor to saturation, q_{new}. At the same time, the temperature will rise from T_{old} to T_{new}. This process is modified slightly for the second and third level. At these levels, the possibility is checked of evaporating any precipitated water into the next lower level and letting rain fall to the ground only if the next lower layer thus becomes saturated.

The enforcement of a total convective adjustment on the model is divided into two parts, a parameterized cumulus convection and a dry convective adjustment.

Following a method devised by Arakawa et al. (1969), we considered three types of parameterized cumulus convection. The first type is that occurring between levels 2 and 3 (fig. 11), the second type is that occurring among the levels 1, 2, and 3, and the third type is that occurring between levels 1 and 2. Precipitation may result from types 1 and 2 but not from type 3. Figure 11 schematically illustrates these three types of parameterized convection.

Two parameters used to indicate which type may occur are the energy parameters

$$h = c_p T + gz + Lq \tag{59}$$

and

$$E_n = c_p T + gz + Lq_s. \tag{60}$$

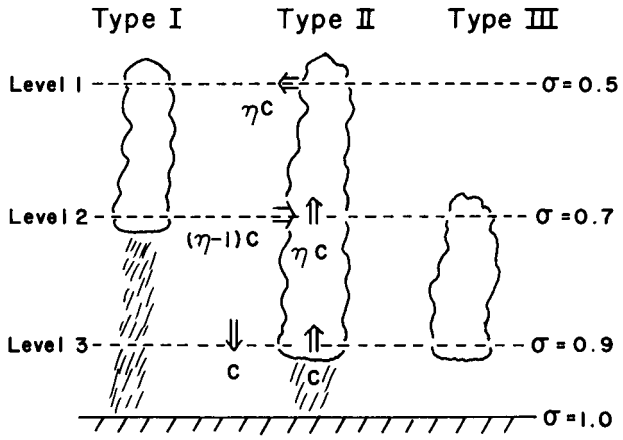

FIGURE 11.—Schematic representation of three types of parameterized cumulus convection where η is the entrainment coefficient and C is the convective mass flux.

E_n is constant along a moist pseudo-adiabat and $(c_pT + gz)$ is constant along a dry adiabat. Thus, comparison of h and E_n for various levels allows for a sufficient test of conditional instability.

Type 1 convection will occur if

$$h_2 > E_{n3}. \tag{61}$$

If $E_{n2} = E_{n3}$, a moist adiabatic lapse rate would exist between levels 2 and 3. Since $h_2 < E_{n2}$, inequality (61) implies that a conditionally unstable lapse rate exists. Furthermore, inequality (61) can be rewritten

$$q_2 > \frac{(E_{n3} - c_p T_2 - g z_2)}{L}. \tag{62}$$

Type 2 convection will occur if

$$E_{n3} > h_2, \qquad h_1 > E_{n3}. \tag{63}$$

Conditional instability does not exist here between levels 2 and 3 but does exist between levels 1 and 3.

Finally, type 3 convection will occur if

$$E_{n3} > h_1 > E_{n2}. \tag{64}$$

Levels 1 and 2 are conditionally unstable; levels 2 and 3 are not.

The procedure now is to write down equations describing the budget for the moisture and the potential temperature for each type of convection. Before this can be done, the energy budget for the lower part of the cloud is considered, neglecting any accumulated storage of energy within the cloud.

We use type 2 as an example. When the entrainment coefficient, η, is greater than 1, entrainment exists and the parameter E_n in the clouds, E_{nc}, is given by a mixing of h_1 and h_2 in the lower part of the clouds as follows:

$$E_{nc} = h_2 + \frac{1}{\eta}(h_1 - h_2) \tag{65}$$

because h is approximately conserved with respect to an

air parcel. At level three,

$$E_{nc}=c_pT_{c3}+gz_3+Lq_s(T_{c3}) \tag{66}$$

whereas for the environmental air,

$$E_{n3}=c_pT_3+gz_3+Lq_s(T_3). \tag{67}$$

Therefore,

$$T_{c3}-T_3=\frac{1}{1+\frac{L}{c_p}\left(\frac{\partial q_s}{\partial T}\right)_3}\left(\frac{E_{nc}-E_{n3}}{c_p}\right). \tag{68}$$

For type 1 and 3 convection, E_{nc} is given by h_2 and h_1 respectively. From eq (68), one can obtain approximately

$$q_{c3}-q_{s3}=\frac{\gamma_3}{1+\gamma_3}\left(\frac{E_{nc}-E_{n3}}{L}\right) \tag{69}$$

where

$$\gamma_3\equiv\frac{L}{c_p}\left(\frac{\partial q_s}{\partial T}\right)_3. \tag{70}$$

For types 1 and 2, the *convective* terms in the moisture and potential temperature budget can be written in flux form

$$\frac{\Delta p_3}{g}\frac{\partial q_3}{\partial t}=\eta C\left[q_{s3}+\frac{\gamma_3}{1+\gamma_3}\left(\frac{E_{nc}-E_{n3}}{L}\right)-\frac{q_3+q_2}{2}\right], \tag{71}$$

$$\frac{\Delta p_2}{g}\frac{\partial q_2}{\partial t}=\eta C\left[\frac{q_3-q_2}{2}+\frac{1}{\eta}\left(\frac{q_2-q_1}{2}\right)\right], \tag{72}$$

$$\frac{\Delta p_1}{g}\frac{\partial q_1}{\partial t}=C\left(\frac{q_2-q_1}{2}\right) \quad \text{(type 2 only)}, \tag{73}$$

$$\frac{\Delta p_3}{g}\frac{\partial \Theta_3}{\partial t}=\eta C\left(\frac{E_{nc}-E_{n3}}{1+\gamma_3}+\frac{\Theta_3-\Theta_2}{2}\right), \tag{74}$$

$$\frac{\Delta p_2}{g}\frac{\partial \Theta_2}{\partial t}=\eta C\left[\frac{\Theta_3-\Theta_2}{2}+\frac{1}{\eta}\left(\frac{\Theta_2-\Theta_1}{2}\right)\right], \tag{75}$$

and

$$\frac{\Delta p_1}{g}\frac{\partial \Theta_1}{\partial t}=C\left(\frac{\Theta_2-\Theta_1}{2}\right) \quad \text{(type 2 only)}. \tag{76}$$

For type 3 convection,

$$\frac{\Delta p_2}{g}\frac{\partial q_2}{\partial t}=C\left(\frac{q_1-q_2}{2}\right)=-\frac{\Delta p_1}{g}\frac{\partial q_1}{\partial t} \tag{77}$$

and

$$\frac{\Delta p_2}{g}\frac{\partial \Theta_2}{\partial t}=C\left(\frac{\Theta_1-\Theta_2}{2}\right)=-\frac{\Delta p_1}{g}\frac{\partial \Theta_1}{\partial t} \tag{78}$$

where $\Theta\equiv c_pT+gz$ and C is the convective mass flux.

For type 1 convection, it can be shown by manipulation of the above equations that

$$\eta C=-\frac{\Delta p}{g\tau}\left(\frac{1+\gamma_3}{2+\gamma_3}\right)\frac{(h_2-E_{n3})}{\left[(h_2-E_{n3})+\left(\frac{1+\gamma_3}{2}\right)(\Theta_3-\Theta_2)\right]} \tag{79}$$

where τ is the time scale for the convective process (1 hr is used).

For type 2 convection, a value of 1°C was used for $(T_{c3}-T_3)$ though tests with values as low as 0.1°C give nearly the same result. Therefore, from eq (65) and (68),

$$\eta=\frac{(h_1-h_2)}{E_{n3}+c_p(1+\gamma_3)-h_2}, \tag{80}$$

and it can be shown that

$$C=-\frac{\Delta p}{g\tau}\frac{(h_1-E_{n3})}{\left[\eta(1+\gamma_3)\left(c_p+\frac{\Theta_3+\Theta_2}{2}\right)+\left(\frac{h_1-h_2}{2}\right)\right]}. \tag{81}$$

For the type 3 convection, one can obtain

$$C=-\frac{1}{\tau}\frac{(h_1-E_2)}{\left[\left(\frac{2+\gamma_2}{2}\right)(\Theta_1-\Theta_2)-L\left(\frac{q_1-q_2}{2}\right)\right]}. \tag{82}$$

Finally, for the dry convective adjustment, the vertical lapse rate of potential temperature is checked to assure that it not be allowed to become negative. If it does, it must be adjusted in such a manner that the mean potential temperature in the vertical is conserved. This may lead, therefore, to some redistribution of heat in the vertical especially between the lower levels of the model during daylight hours over land areas.

REFERENCES

Arakawa, Akio, "Computational Design for Long-Term Numerical Integration of the Equations of Fluid Motion: Two-Dimensional Incompressible Flow. Part I," *Journal of Computational Physics*, Vol. 1, No. 1, Academic Press, Inc., New York, N.Y., Jan. **1966**, pp. 119–143.

Arakawa, Akio, Katayama, Akira, and Mintz, Yale, "Numerical Simulation of the General Circulation of the Atmosphere," *Proceedings of the WMO/IUGG Symposium on Numerical Weather Prediction, Tokyo, Japan, November 26–December 4, 1968*, Japan Meteorological Agency, Tokyo, Mar. **1969**, pp. IV–1—IV–14.

Beckett, William, Kesel, Phillip, Winninghoff, Francis J., Wolff, Paul, and Morenoff, E., "Four-Way Parallel Processor Partition of an Atmospheric Primitive Equation Prediction Model," *Proceedings of the AFIPS Spring Joint Computer Conference, Atlantic City, New Jersey, May 18–20, 1971*, Vol. 38, American Federation of Information Processing Societies Press, Montvale, N.J., **1971**, pp. 39–48.

Danard, Maurice B., "A Simple Method of Including Longwave Radiation in a Tropospheric Numerical Prediction Model," *Monthly Weather Review*, Vol. 97, No. 1, Jan. **1969**, pp. 77–85.

Dickson, Robert R., and Posey, Julian, "Maps of Snow-Cover Probability for the Northern Hemisphere," *Monthly Weather Review*, Vol. 95, No. 6, June **1967**, pp. 347–353.

Haltiner, George J., *Numerical Weather Prediction*, John Wiley & Sons, Inc., New York, N.Y., **1971**, 317 pp.

Joseph, Joachim H., "Calculation of Radiative Heating in Numerical General Circulation Models," *Numerical Simulation of Weather and Climate Technical Report* No. 1, Department of Meteorology, University of California, Los Angeles, Aug. 1, **1966**, 60 pp.

Kuhn, Peter M., "Soundings of Observed and Computed Infrared Flux," *Journal of Geophysical Research*, Vol. 68, No. 5, Mar. **1963**, pp. 1415–1420.

Kurihara, Yoshio, "Correspondence—Note on Finite Difference Expressions for the Hydrostatic Relation and Pressure Gradient Force," *Monthly Weather Review*, Vol. 96, No. 9, Sept. **1968**, pp. 654–656.

Langlois, W. E., and Kwok, C. W., "Description of the Mintz-Arakawa Numerical General Circulation Model," *Numerical Simulation of Weather and Climate Technical Report* No. 3, Department of Meteorology, University of California, Los Angeles, **1969**, 95 pp.

Manabe, Syukuro, and Möller, Fritz, "On the Radiative Equilibrium and Heat Balance of the Atmosphere," *Monthly Weather Review*, Vol. 89, No. 12, Dec. **1961**, pp. 503–532.

Phillips, Norman A., "A Coordinate System Having Some Special Advantages for Numerical Forecasting," *Journal of Meteorology*, Vol. 14, No. 4, Apr. **1957**, pp. 184–185.

Sellers, William D., *Physical Climatology*, The University of Chicago Press, Ill., **1965**, 272 pp.

Shuman, Frederick G., and Hovermale, John B., "An Operational Six-Layer Primitive Equation Model," *Journal of Applied Meteorology*, Vol. 7, No. 4, Aug. **1968**, pp. 525–547.

Smagorinsky, Joseph, "On the Dynamical Prediction of Large-Scale Condensation by Numerical Methods," *Geophysical Monograph* No. 5, American Geophysical Union, Washington, D.C., **1960**, pp. 71–78.

Smagorinsky, Joseph, Manabe, Syukuro, and Holloway, J. Leith, Jr., "Numerical Results From a Nine-Level General Circulation Model of the Atmosphere," *Monthly Weather Review*, Vol. 93, No. 12, Dec. **1965**, pp. 727–768.

Winninghoff, Francis J., "On the Adjustment Toward a Geostrophic Balance in a Simple Primitive Equation Model With Application to the Problems of Initialization and Objective Analysis," Ph. D thesis, University of California, Los Angeles, Dec. **1968**, 161 pp

[*Received March 29, 1971; revised December 27, 1971*]

CORRECTION NOTICE

Vol. 100, No. 2, Feb. 1972, p. 90, left col. line 5: "latter" is to be read instead of "potential evaporation rate."